

Effects of hydrodynamic and initial longitudinal fluctuations on rapidity decorrelation of collective flow

Azumi Sakai^a, Koichi Murase^{b,c}, Tetsufumi Hirano^a

^a *Department of Physics, Sophia University, Tokyo 102-8554, Japan*

^b *Yukawa Institute for Theoretical Physics, Kyoto University, Kyoto 606-8502, Japan*

^c *Center for High Energy Physics, Peking University, Beijing 100871, China*

Abstract

We investigate the interplay between hydrodynamic fluctuations and initial longitudinal fluctuations for their effects on the rapidity decorrelation of collective flow in high-energy nuclear collisions. We use a (3+1)-dimensional integrated dynamical model in which we combine initial conditions with longitudinal fluctuations, fluctuating hydrodynamics and hadronic cascades. We analyse the factorisation ratio in the longitudinal direction to study the effect of these fluctuations on the rapidity decorrelation. We find an essential difference between the effects of the hydrodynamic fluctuations and the initial longitudinal fluctuations in the centrality dependence of the factorisation ratios. A combination of the hydrodynamic fluctuations and the initial longitudinal fluctuations leads to reproduction of the centrality dependence of the second-order factorisation ratio, $r_2(\eta_p^a, \eta_p^b)$, measured by the CMS Collaboration. Our model also qualitatively describes the centrality dependence of the third-order factorisation ratio, $r_3(\eta_p^a, \eta_p^b)$. These results demonstrate the importance of the hydrodynamic fluctuations, as well as the initial longitudinal fluctuations, in understanding the longitudinal dynamics of high-energy nuclear collision reactions.

Keywords: quark–gluon plasma, relativistic fluctuating hydrodynamics, factorisation ratios

Email addresses: a-sakai-s4d@eagle.sophia.ac.jp (Azumi Sakai),
koichi.murase@yukawa.kyoto-u.ac.jp (Koichi Murase), hirano@sophia.ac.jp
(Tetsufumi Hirano)

High-energy nuclear collision experiments performed at the Relativistic Heavy Ion Collider (RHIC) at Brookhaven National Laboratory and the Large Hadron Collider (LHC) at CERN aim at understanding the bulk and transport properties of the deconfined nuclear matter, the quark–gluon plasma (QGP) [1]. One of the major discoveries at RHIC is the large magnitude of the second-order azimuthal anisotropy [2, 3, 4, 5, 6, 7], also known as the elliptic flow [8]. The elliptic flow turned out to be consistent with the results from ideal hydrodynamic models [9, 10, 11, 12, 13, 14], which led to the development of later sophisticated dynamical models based on hydrodynamics including viscosity [15, 16, 17, 18, 19, 20, 21, 22] and hydrodynamic fluctuations [23, 24, 25, 26, 27, 28]. The large elliptic flow was observed also at LHC [29, 30, 31, 32], and later, higher-order anisotropic flows have been systematically measured at RHIC [33, 34] and LHC [30, 35, 36].

To understand collective flow phenomena more comprehensively, the correlation of the anisotropic flow has been studied through, e.g., the factorisation ratio which was initially proposed as a function of the transverse momentum [37] and extended in the longitudinal direction [38]. The longitudinal factorisation ratios are widely measured in experiments [38, 39, 40, 41, 42], where the rapidity decorrelation is observed as the factorisation breakdown. The longitudinal dynamics carries more information on the model-specific fluctuations that are independent of the geometric origin of the initial nucleon distributions, and thus the longitudinal factorisation ratio is one of the good measures for the model discrimination. These factorisation ratios are studied with various initialisation models [43, 44, 45, 46, 47, 48] and longitudinal-fluctuation mechanisms [49, 50, 51, 52, 25, 53, 54, 28]. Although these models exhibit the factorisation breakdown, none has quantitatively described all the measurements, including the centrality dependence, different harmonic orders and the collision energy dependence, in a single model setup. In our previous study with the fluctuating hydrodynamic model [28], we have shown the significance of the hydrodynamic fluctuations in understanding the longitudinal dynamics while the initial fluctuations of longitudinal profiles were missing there. Hydrodynamic fluctuations are thermal fluctuations of the hydrodynamic description whose power is determined by the fluctuation–dissipation relation [55, 56, 57, 58, 59, 60, 61]. Besides, the initial-state longitudinal fluctuations also play an important role in the final-state decorrelations [49, 50, 51, 52, 53, 54]. Therefore, in this Letter, we investigate both effects of the longitudinal fluctuations in the initial stage and the hydrodynamic fluctuations in the hydrodynamic stage on the rapid-

ity decorrelation.

In this Letter, we employ the integrated dynamical model with hydrodynamic fluctuations [62, 28], where the causal fluctuating hydrodynamic code `rfh` [24] is combined with the initialisation model and the cascade model `JAM` [63] with the prescription described in Ref. [64]. For the initialisation model, we newly implement the initial longitudinal fluctuations in the Monte-Carlo version of the Glauber model. The constitutive equations for the shear-stress tensor, $\pi^{\mu\nu}$, in the causal fluctuating hydrodynamics are chosen as [24, 61, 65]

$$\tau_\pi \Delta^{\mu\nu}{}_{\alpha\beta} u^\lambda \partial_{;\lambda} \pi^{\alpha\beta} + \pi^{\mu\nu} \left(1 + \frac{4}{3} \tau_\pi \partial_{;\lambda} u^\lambda \right) = 2\eta \Delta^{\mu\nu}{}_{\alpha\beta} \partial^{;\alpha} u^\beta + \xi^{\mu\nu}, \quad (1)$$

where η and τ_π are the shear viscosity and the relaxation time, respectively. The tensor $\Delta^{\mu\nu} = g^{\mu\nu} - u^\mu u^\nu$ is a projector for four-vectors onto the components transverse to the flow velocity u^μ where the sign convention for the metric is $g_{\mu\nu} = \text{diag}(+, -, -, -)$. The tensor $\Delta^{\mu\nu}{}_{\alpha\beta} = \frac{1}{2} (\Delta^\mu{}_\alpha \Delta^\nu{}_\beta + \Delta^\mu{}_\beta \Delta^\nu{}_\alpha) - \frac{1}{3} \Delta^{\mu\nu} \Delta_{\alpha\beta}$ is a projector for second-rank tensors onto the symmetric and traceless components transverse to the flow velocity. The symbol $\partial_{;\mu}$ denotes the covariant derivative. The noise term $\xi^{\mu\nu}$ represents the hydrodynamic fluctuations and obeys the fluctuation–dissipation relation. In the Milne coordinates $(\tau, \eta_s, \mathbf{x}_\perp) := (\sqrt{t^2 - z^2}, \tanh^{-1}(z/t), x, y)$, the fluctuation–dissipation relation is written as

$$\langle \xi^{\mu\nu}(\tau, \eta_s, \mathbf{x}_\perp) \xi^{\alpha\beta}(\tau', \eta'_s, \mathbf{x}'_\perp) \rangle = 4\eta T \Delta^{\mu\nu\alpha\beta} \cdot \frac{1}{\tau} \delta(\tau - \tau') \delta(\eta_s - \eta'_s) \delta^{(2)}(\mathbf{x}_\perp - \mathbf{x}'_\perp), \quad (2)$$

where T is the temperature, and the angle brackets mean ensemble average, which is associated with the event average in the context of the high-energy nuclear collisions. Here, the Lorentz indices in Eq. (2) represent τ , η_s , x or y . In the actual calculations, we introduce the spatial cutoff to the hydrodynamic fluctuations by convoluting the Gaussian profile of widths λ_η and λ_\perp in the longitudinal and transverse directions, respectively. This effectively replaces the spatial delta function in Eq. (2) by the Gaussian of width $2\lambda_\eta$ and $2\lambda_\perp$. Smaller cutoff parameters result in larger effects of the hydrodynamic fluctuations. It is noted here that these cutoff parameters are specified in the coordinate space rather than in the momentum space in this Letter.

In the hydrodynamic simulations, the initial entropy density distributions, $s(\tau_0, \eta_s, \mathbf{x}_\perp)$, are needed at a fixed initial time τ_0 . For the event-by-event initial profiles, we utilise the Monte-Carlo version of the Glauber

(MC-Glauber) model [66, 64] combined with a general-purpose event generator, PYTHIA [67]. For each binary collision, we generate hadrons in a p+p collision using PYTHIA. Here, we neglect the difference between p+p and p+n / n+n binary collisions that happen in real nuclear collisions for simplicity. If we would simply sum up all the hadrons from the binary collisions, the multiplicity would scale with the number of the binary collisions, N_{coll} , which would be plausible only in high-transverse-momentum (high- p_T) regions. On the other hand, yields of low-transverse-momentum (low- p_T) hadrons are expected to scale with the number of participants, N_{part} . To embody this scaling behaviour throughout the whole transverse momentum regions, we perform a rejection sampling for these generated hadrons with the momentum-dependent acceptance probability $w(Y, p_T)$ [68, 69]:

$$w(p_T, Y) = w(Y) \times \frac{1}{2} \left[1 - \tanh \left(\frac{p_T - p_{T0}}{\Delta p_T} \right) \right] + \frac{1}{2} \left[1 + \tanh \left(\frac{p_T - p_{T0}}{\Delta p_T} \right) \right], \quad (3)$$

$$w(Y) = \frac{Y_b + Y}{2Y_b} \frac{1}{n_A} + \frac{Y_b - Y}{2Y_b} \frac{1}{n_B}. \quad (4)$$

Here, p_T and Y are the transverse momentum and the rapidity of the hadron, respectively. We introduce the parameters p_{T0} and Δp_T to smoothly separate low- and high- p_T regions into the first and second terms, respectively, so that the total number of accepted hadrons scales with N_{part} (N_{coll}) in the low- (high-) p_T region. The symbol Y_b denotes the beam rapidity, and n_A (n_B) is the number of binary collisions that the nucleon of the current binary collision at positive (negative) beam rapidity experiences. The scaling with N_{part} is implemented by the function $w(Y)$. This function $w(Y)$ also brings rapidity-dependent yields of hadrons [70, 71, 72], which shares the idea with that of the wounded nucleon model [73]. The free parameters p_{T0} and Δp_T are later tuned to reproduce the centrality dependence of the charged-particle multiplicity.

We assume the initial entropy-density distribution is proportional to the number distribution of the accepted hadrons:

$$s(\tau_0, \eta_s, \mathbf{x}_\perp) = \frac{K}{\tau_0} \sum_i \frac{1}{\sqrt{2\pi\sigma_\eta^2}} \frac{1}{2\pi\sigma_\perp^2} \exp \left[-\frac{(\mathbf{x}_\perp - \mathbf{x}_\perp^i)^2}{2\sigma_\perp^2} - \frac{(\eta_s - \eta_s^i)^2}{2\sigma_\eta^2} \right], \quad (5)$$

where the model parameter K controls the overall normalisation. The longitudinal position of the i -th hadron at the initial time τ_0 is determined as

$\eta_s^i = Y^i$. The initial transverse position of the i -th hadron \mathbf{x}_\perp^i is randomly sampled in the uniform disk of the radius $\sqrt{\sigma_{\text{in}}^{\text{NN}}/\pi}$ and the centre $\mathbf{x}_{\text{centre}}^i$. Here, $\sigma_{\text{in}}^{\text{NN}}(\sqrt{s_{\text{NN}}})$ is the inelastic-scattering cross section of nucleons, and we place the centre at

$$\mathbf{x}_{\text{centre}}^i = \frac{\mathbf{x}_\perp^{i,\text{A}} + \mathbf{x}_\perp^{i,\text{B}}}{2} + \frac{\mathbf{x}_\perp^{i,\text{A}} - \mathbf{x}_\perp^{i,\text{B}}}{2Y_{\text{b}}} \eta_s^i, \quad (6)$$

where $\mathbf{x}_\perp^{i,\text{A}}$ ($\mathbf{x}_\perp^{i,\text{B}}$) is the position of the associated nucleon at the positive (negative) beam rapidity. Here we assumed that a hadron is produced around a line in the Milne coordinates connecting the two nucleons of the associated binary collision.

We put the Bjorken scaling solution [74] for the initial flow velocity $u^\mu(\tau_0, \eta_s, \mathbf{x}_\perp) = (u^\tau, u^{\eta_s}, u^x, u^y) = (1, 0, 0, 0)$, which means that we ignore the fluctuations of initial flows in this study. For the equation of state, we employ a lattice-based model, *s95p-v1.1* [75], in which the list of hadrons in the hadron resonance gas model is taken from the cascade model JAM [63]. At the switching temperature T_{sw} , we change the description from the macroscopic hydrodynamics to the microscopic kinetic theory using the Cooper–Frye formula [76]. The subsequent space-time evolution of hadrons is described by using the cascade model JAM [63]. Further details of the integrated dynamical model with fluctuating hydrodynamics can be found in Refs. [24, 61, 28].

Using this model, we perform simulations for Pb+Pb collisions at $\sqrt{s_{\text{NN}}} = 2.76$ TeV. For the reference setup to see the effects of hydrodynamic fluctuations, we also perform the simulations of viscous hydrodynamics by turning off the hydrodynamic fluctuations. For each hydrodynamic model (fluctuating hydrodynamics and viscous hydrodynamics), we gain 4 000 minimum-bias hydrodynamic events. For each hydrodynamic event, we perform 100 independent particlisation and hadronic cascade simulations to reduce the computational cost. In total we obtain the 400 000 ($= 4\,000 \times 100$) events for the subsequent analyses.

Let us here summarise the parameters of the present study. Following the previous calculations [62, 64], we set the specific shear viscosity $\eta/s = 1/4\pi$ [77], the relaxation time $\tau_\pi = 3/4\pi T$ [78, 65], the initial proper time $\tau_0 = 0.6$ fm and the switching temperature $T_{\text{sw}} = 155$ MeV. We fix the widths of the hadron profile as $\sigma_\perp = 0.3$ fm and $\sigma_\eta = 0.3$ at present. We tune initial parameters K , $p_{\text{T}0}$ and Δp_{T} for each hydrodynamic model to reproduce centrality dependence of charged-particle multiplicity measured

by the ALICE Collaboration [79]. For the fluctuating hydrodynamics, we tune the cutoff parameters λ_{\perp} and λ_{η} to roughly reproduce the factorisation ratio $r_2(\eta_p^a, \eta_p^b)$ measured by the CMS Collaboration [38]. In the present study we assume $\lambda_{\perp}/\text{fm} = \lambda_{\eta}$ for simplicity. These parameters for each hydrodynamic model are summarised in Table 1. The parameter K controls

Table 1: Parameters in hydrodynamic models

Model	λ_{\perp} (fm)	λ_{η}	K	p_{T0} (GeV)	Δp_T (GeV)
Viscous hydro	N/A	N/A	4.8	1.75	1.0
Fluc. hydro- $\lambda_{2.0}$	2.0	2.0	4.8	1.80	1.0

the overall magnitude of multiplicity per participant pair. On the other hand, the parameter p_{T0} controls not only the overall magnitude but also the slope of multiplicity per participant pair. The parameter p_{T0} is slightly larger in fluctuating hydrodynamics because the entropy production in the hydrodynamic stage in the peripheral collisions is larger with fluctuating hydrodynamics than with viscous hydrodynamics [28].

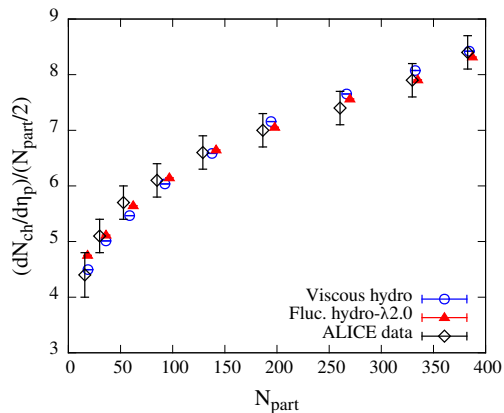


Figure 1: (Colour Online) Charged-hadron multiplicity normalised by the number of the participant pair $(dN_{\text{ch}}/d\eta_p)/(N_{\text{part}}/2)$, as a function of the number of participants. Results from viscous hydrodynamics with initial longitudinal fluctuations (open circle) and fluctuating hydrodynamics with initial longitudinal fluctuations (filled triangle) are compared with experimental data (open diamond) obtained by the ALICE Collaboration [79].

Figure 1 shows N_{part} dependence of charged-hadron multiplicity $dN_{\text{ch}}/d\eta_p$ per participant pair $N_{\text{part}}/2$ at midrapidity $|\eta_p| < 0.5$ in Pb+Pb collisions

at $\sqrt{s_{\text{NN}}} = 2.76$ TeV. Within our initialisation model, the violation of N_{part} scaling in multiplicity in Fig. 1 is described by the initial (semi-)hard components introduced through the acceptance probability Eq. (3).

The initial longitudinal fluctuations and the hydrodynamic fluctuations, which follow Eqs. (1) and (5), respectively, randomly disturb the correlations such as alignment of the event planes along rapidity. We analyse factorisation ratios [37] to see the effects of these fluctuations on (de-)correlation of event-plane angles along rapidity. The factorisation ratio in the longitudinal direction is defined as

$$r_n(\eta_p^a, \eta_p^b) = \frac{V_{n\Delta}(-\eta_p^a, \eta_p^b)}{V_{n\Delta}(\eta_p^a, \eta_p^b)}, \quad V_{n\Delta} = \langle \cos(n\Delta\phi) \rangle. \quad (7)$$

Here $V_{n\Delta}$ is the Fourier coefficients of two-particle correlation functions at the n -th order and $\Delta\phi$ is a difference of the azimuthal angles between two charged hadrons in separated pseudorapidity regions, η_p^a and η_p^b . If one could factorise the two-particle correlation functions in the denominator and numerator in Eq. (7) into two anisotropic flows with corresponding momentum regions, e.g., $V_{n\Delta}(\eta_p^a, \eta_p^b) = v_2(\eta_p^a)v_2(\eta_p^b)$, the resultant factorisation ratio would be equal to unity in symmetric collisions. Contrarily, when the event-plane angle and the flow magnitude fluctuate as functions of pseudorapidity, the ratio becomes smaller than unity in general because one cannot factorise the two-particle correlation functions. This decrease of the factorisation ratio from the unity is called the flow decorrelation in the longitudinal direction. In the following analyses, the two-particle correlation function is calculated by changing the rapidity region of the hadrons within $0 < \eta_p^a < 2.5$ while fixing the region of the reference hadrons to be $3.0 < \eta_p^b < 4.0$ following the experimental setup by the CMS Collaboration [38].

Figure 2 shows the factorisation ratio in the longitudinal direction, $r_2(\eta_p^a, \eta_p^b)$, in Pb+Pb collisions at $\sqrt{s_{\text{NN}}} = 2.76$ TeV for 0–5% and 20–30% centralities compared with the experimental data by the CMS Collaboration [38]. The cutoff parameters $\lambda_{\perp}/\text{fm} = \lambda_{\eta} = 2.0$ in Table 1 have been here determined to reproduce the experimental results of $r_2(\eta_p^a, \eta_p^b)$ of the 20–30% centrality. These values are larger than $\lambda_{\perp}/\text{fm} = \lambda_{\eta} = 1.0$ and 1.5 (parameters $\lambda_{1.0}$ and $\lambda_{1.5}$, respectively) of the previous work [28]. This is because the effect of newly introduced initial longitudinal fluctuations needs to be compensated by reducing the effect of the hydrodynamic fluctuations to keep the factorisation ratios the same.

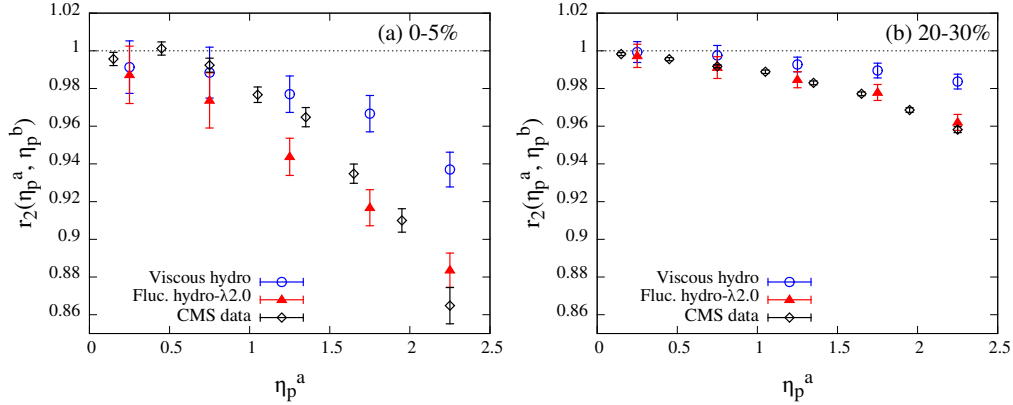


Figure 2: Factorisation ratio $r_2(\eta_p^a, \eta_p^b)$ in Pb+Pb collisions at $\sqrt{s_{\text{NN}}} = 2.76$ TeV for (a) 0–5% and (b) 20–30% centralities. The rapidity region for reference is $3.0 < \eta_p^b < 4.0$. Open circles and filled triangles are results from the viscous and fluctuating hydrodynamic models, respectively. The experimental data of $r_2(\eta_p^a, \eta_p^b)$ from the CMS Collaboration [38] are shown by open diamonds.

The experimental data is close to unity at small η_p^a and decreases with increasing η_p^a . The factorisation ratio $r_2(\eta_p^a, \eta_p^b)$ from the viscous hydrodynamic model with initial longitudinal fluctuations decreases with increasing η_p^a . However, the decorrelation is weaker than experimental data in particular at the large rapidity gap $\eta_p^a \sim 1.5$ – 2.5 . Since viscous hydrodynamics tends to keep the long-range correlation in the rapidity direction [28], the decreasing behaviour of $r_2(\eta_p^a, \eta_p^b)$ can be attributed to the initial longitudinal fluctuations [54, 51, 50, 52, 53]. In the fluctuating hydrodynamic model, the decorrelation is stronger than in the viscous hydrodynamic model, which is the same trend as in the previous analysis without the initial longitudinal fluctuations in Ref. [28].

Figures 3 (a) and (b) compare the centrality dependence of $r_2(\eta_p^a, \eta_p^b)$ from hydrodynamic models with and without initial longitudinal fluctuations, respectively. We find that the experimental data of the centrality dependence of $r_2(\eta_p^a, \eta_p^b)$ can only be reproduced by the model with both the hydrodynamic fluctuations and the initial longitudinal fluctuations. This can be understood from the different centrality dependence between the effects of the initial longitudinal fluctuations and the hydrodynamic fluctuations.

Within our model, the genuine initial longitudinal fluctuations tend to decrease $r_2(\eta_p^a, \eta_p^b)$ in central collisions (particularly in 0–10% centrality), as

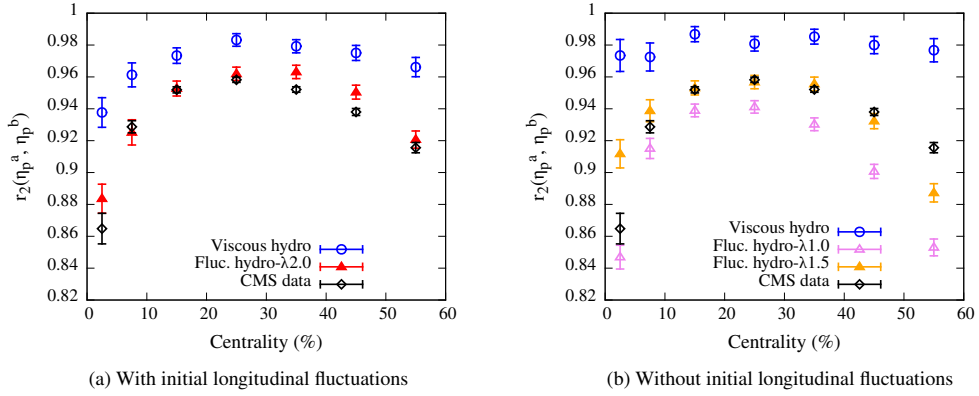


Figure 3: (Colour Online) Centrality dependence of factorisation ratio $r_2(\eta_p^a, \eta_p^b)$ in Pb+Pb collisions at $\sqrt{s_{NN}} = 2.76$ TeV. The rapidity regions of two-particle correlation functions are taken as $2.0 < \eta_p^a < 2.5$ and $3.0 < \eta_p^b < 4.0$. (a) The results from hydrodynamic models with initial longitudinal fluctuations are compared with the experimental data [38]. (b) The results from hydrodynamic model without initial longitudinal fluctuations (taken from Fig. 6 in Ref. [28]) are also shown for comparison. In the right panel (b), we show the result from viscous hydrodynamics and two results from the fluctuating hydrodynamics with different cutoff parameters $\lambda 1.5$ (filled triangle) and $\lambda 1.0$ (open triangle), which correspond to the cutoff $\lambda_{\perp}/\text{fm} = \lambda_{\eta} = 1.5$ and 1.0 , respectively [see Ref. [28] for the other parameters used in panel (b)]. The symbols are the same as in Fig. 2 for other plots.

seen in the open circles in Fig. 3 (a). This is because the flow correlation along the rapidity direction can be easily broken in the central collisions as the magnitude of the elliptic flow driven by the collision geometry is small there. On the other hand, the genuine hydrodynamic fluctuations tend to decrease $r_2(\eta_p^a, \eta_p^b)$ in both central collisions (0–10% centrality) and peripheral collisions (40–60% centrality) as seen in Fig. 3 (b). The mechanism of the decorrelation in central collisions is the same as with the initial longitudinal fluctuations. The decorrelation in the peripheral collisions can be attributed to the nature of the hydrodynamic fluctuations being significant in small and short-lived systems, i.e., the magnitude of the averaged thermal fluctuations at the linear order scales as $(Vt)^{-1/2}$ where V and t are the typical volume and lifetime of the system. If we do not take account of initial longitudinal fluctuations, the factorisation ratio $r_2(\eta_p^a, \eta_p^b)$ of the experimental data can be well fitted by parameter $\lambda 1.0$ (open triangles) and $\lambda 1.5$ (filled triangles) in central collisions and peripheral collisions, respectively, but the overall centrality dependence cannot be reproduced by a single cutoff parameter.

Neither the fluctuating hydrodynamics without the initial longitudinal fluctuations with fixed λ parameters nor the viscous hydrodynamics with the initial longitudinal fluctuations can reproduce the centrality dependence of the experimental data. Thus we conclude that *both the initial longitudinal fluctuations and the hydrodynamic fluctuations* must be taken into consideration in understanding the centrality dependence of the factorisation ratios.

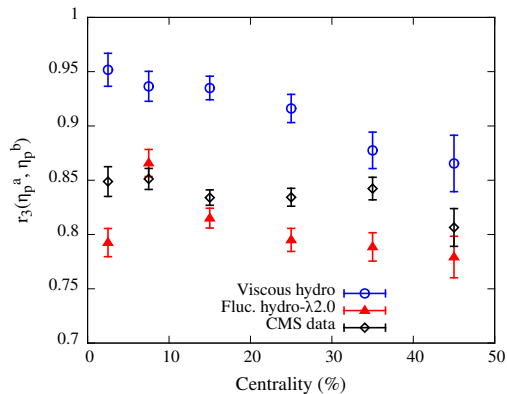


Figure 4: (Colour Online) Centrality dependence of factorisation ratio $r_3(\eta_p^a, \eta_p^b)$ in Pb+Pb collisions at $\sqrt{s_{\text{NN}}} = 2.76$ TeV. The rapidity regions of two-particle correlation functions are taken as $2.0 < \eta_p^a < 2.5$ and $3.0 < \eta_p^b < 4.0$. The symbols are the same as in Fig. 1. The experimental data are obtained by the CMS Collaboration [38].

Figure 4 shows the centrality dependence of $r_3(\eta_p^a, \eta_p^b)$ in Pb+Pb collisions at $\sqrt{s_{\text{NN}}} = 2.76$ TeV. The factorisation ratio $r_3(\eta_p^a, \eta_p^b)$ in experimental data depends mildly on centrality. This is because the triangular flow is dominated by fluctuations in symmetric collision systems. The factorisation ratio $r_3(\eta_p^a, \eta_p^b)$ from the viscous hydrodynamic model with initial longitudinal fluctuations decreases with increasing centrality percentage and is larger than the experimental data in all centralities. In contrast, $r_3(\eta_p^a, \eta_p^b)$ obtained from the fluctuating hydrodynamic model has less centrality dependence and is also close to experimental data. Although more sophisticated modelling would be required to perfectly reproduce the experimental data of both $r_2(\eta_p^a, \eta_p^b)$ and $r_3(\eta_p^a, \eta_p^b)$ simultaneously, the centrality dependences of $r_2(\eta_p^a, \eta_p^b)$ and $r_3(\eta_p^a, \eta_p^b)$ are better reproduced by including both the hydrodynamic fluctuations and the initial longitudinal fluctuations. These results suggest that considering either the initial longitudinal fluctuations or the hydrodynamic fluctuations is insufficient in understanding the decorrelation of anisotropic flows in the longitudinal directions and thus that considering both simultaneously in a model is important.

In this Letter, we investigated the effects of the longitudinal fluctuations in the initial stage and the hydrodynamic fluctuations in the expansion stage on the longitudinal factorisation ratios to understand the rapidity decorrelation of anisotropic flows. We employed an integrated dynamical model which consists of the initialisation model for fluctuations in both longitudinal and transverse profiles, the hydrodynamic model, `rfh`, for causal hydrodynamic fluctuations and dissipations, and the hadronic cascade model, `JAM`, for the final-state interactions. We performed simulations of Pb+Pb collisions at $\sqrt{s_{\text{NN}}} = 2.76$ TeV using the integrated dynamical model with or without the hydrodynamic fluctuations for comparison. We fixed the model parameters so that our model fairly reproduces the experimental data of the centrality dependence of charged-hadron multiplicity normalised by the number of participants. With these model settings, we calculated the factorisation ratio $r_n(\eta_p^a, \eta_p^b)$ ($n = 2, 3$) in the longitudinal direction and its centrality dependence. We confirmed that both the initial longitudinal fluctuations and the hydrodynamic fluctuations decrease the factorisation ratio, which is consistent with the previous studies. However, we found that the centrality dependence of the effects of hydrodynamic fluctuations is different from those of initial longitudinal fluctuations. We reproduce the centrality dependence of the factorisation ratio at the second order, $r_2(\eta_p^a, \eta_p^b)$, from the CMS collaboration only after including both the initial longitudinal and the hydrodynamic

fluctuations. We also qualitatively described the centrality dependence of the factorisation ratio at the third order, $r_3(\eta_p^a, \eta_p^b)$, with these two fluctuations. These analyses show that incorporating both the initial longitudinal and the hydrodynamic fluctuations simultaneously in a dynamical model is the key to quantitatively understanding the decorrelation dynamics in the longitudinal direction.

Acknowledgement

This work was supported by JSPS KAKENHI Grant Numbers JP18J22227 (A.S.) and JP19K21881 (T.H.). K.M. was supported by the NSFC under Grant No. 11947236.

References

- [1] K. Yagi, T. Hatsuda, Y. Miake, Quark-gluon plasma: From big bang to little bang, *Camb. Monogr. Part. Phys. Nucl. Phys. Cosmol.* 23 (2005) 1–446.
- [2] K. H. Ackermann, et al., Elliptic flow in Au + Au collisions at $(S(NN))^{1/2} = 130$ GeV, *Phys. Rev. Lett.* 86 (2001) 402–407. [arXiv:nucl-ex/0009011](#), [doi:10.1103/PhysRevLett.86.402](#).
- [3] C. Adler, et al., Identified particle elliptic flow in Au + Au collisions at $s(NN)^{1/2} = 130$ -GeV, *Phys. Rev. Lett.* 87 (2001) 182301. [arXiv:nucl-ex/0107003](#), [doi:10.1103/PhysRevLett.87.182301](#).
- [4] J. Adams, et al., Particle type dependence of azimuthal anisotropy and nuclear modification of particle production in Au + Au collisions at $s(NN)^{1/2} = 200$ -GeV, *Phys. Rev. Lett.* 92 (2004) 052302. [arXiv:nucl-ex/0306007](#), [doi:10.1103/PhysRevLett.92.052302](#).
- [5] K. Adcox, et al., Flow measurements via two particle azimuthal correlations in Au+Au collisions at $s(NN)^{1/2} = 130$ -GeV, *Phys. Rev. Lett.* 89 (2002) 212301. [arXiv:nucl-ex/0204005](#), [doi:10.1103/PhysRevLett.89.212301](#).
- [6] S. S. Adler, et al., Elliptic flow of identified hadrons in Au+Au collisions at $s(NN)^{1/2} = 200$ -GeV, *Phys. Rev. Lett.* 91 (2003) 182301. [arXiv:nucl-ex/0305013](#), [doi:10.1103/PhysRevLett.91.182301](#).

- [7] B. B. Back, et al., Pseudorapidity and centrality dependence of the collective flow of charged particles in Au+Au collisions at $\sqrt{s}(\text{NN})^{1/2} = 130\text{-GeV}$, *Phys. Rev. Lett.* 89 (2002) 222301. [arXiv:nucl-ex/0205021](#), [doi:10.1103/PhysRevLett.89.222301](#).
- [8] J.-Y. Ollitrault, Anisotropy as a signature of transverse collective flow, *Phys. Rev. D* 46 (1992) 229–245. [doi:10.1103/PhysRevD.46.229](#).
- [9] P. F. Kolb, P. Huovinen, U. W. Heinz, H. Heiselberg, Elliptic flow at SPS and RHIC: From kinetic transport to hydrodynamics, *Phys. Lett. B* 500 (2001) 232–240. [arXiv:hep-ph/0012137](#), [doi:10.1016/S0370-2693\(01\)00079-X](#).
- [10] D. Teaney, J. Lauret, E. V. Shuryak, Flow at the SPS and RHIC as a quark gluon plasma signature, *Phys. Rev. Lett.* 86 (2001) 4783–4786. [arXiv:nucl-th/0011058](#), [doi:10.1103/PhysRevLett.86.4783](#).
- [11] D. Teaney, J. Lauret, E. V. Shuryak, A Hydrodynamic description of heavy ion collisions at the SPS and RHIC (2001). [arXiv:nucl-th/0110037](#).
- [12] P. Huovinen, P. F. Kolb, U. W. Heinz, P. V. Ruuskanen, S. A. Voloshin, Radial and elliptic flow at RHIC: Further predictions, *Phys. Lett. B* 503 (2001) 58–64. [arXiv:hep-ph/0101136](#), [doi:10.1016/S0370-2693\(01\)00219-2](#).
- [13] T. Hirano, Is early thermalization achieved only near mid-rapidity at RHIC?, *Phys. Rev. C* 65 (2002) 011901. [arXiv:nucl-th/0108004](#), [doi:10.1103/PhysRevC.65.011901](#).
- [14] T. Hirano, K. Tsuda, Collective flow and two pion correlations from a relativistic hydrodynamic model with early chemical freezeout, *Phys. Rev. C* 66 (2002) 054905. [arXiv:nucl-th/0205043](#), [doi:10.1103/PhysRevC.66.054905](#).
- [15] H. Song, U. W. Heinz, Causal viscous hydrodynamics in 2+1 dimensions for relativistic heavy-ion collisions, *Phys. Rev. C* 77 (2008) 064901. [arXiv:0712.3715](#), [doi:10.1103/PhysRevC.77.064901](#).

- [16] K. Dusling, D. Teaney, Simulating elliptic flow with viscous hydrodynamics, *Phys. Rev. C* 77 (2008) 034905. [arXiv:0710.5932](#), [doi:10.1103/PhysRevC.77.034905](#).
- [17] M. Luzum, P. Romatschke, Conformal Relativistic Viscous Hydrodynamics: Applications to RHIC results at $s(\text{NN})^{1/2} = 200\text{-GeV}$, *Phys. Rev. C* 78 (2008) 034915, [Erratum: *Phys. Rev. C* 79,039903(2009)]. [arXiv:0804.4015](#), [doi:10.1103/PhysRevC.78.034915](#), [doi:10.1103/PhysRevC.79.039903](#).
- [18] B. Schenke, S. Jeon, C. Gale, (3+1)D hydrodynamic simulation of relativistic heavy-ion collisions, *Phys. Rev. C* 82 (2010) 014903. [arXiv:1004.1408](#), [doi:10.1103/PhysRevC.82.014903](#).
- [19] P. Bozek, M. Chojnacki, W. Florkowski, B. Tomasik, Hydrodynamic predictions for Pb+Pb collisions at $\sqrt{s_{NN}} = 2.76\text{ TeV}$, *Phys. Lett. B* 694 (2011) 238–241. [arXiv:1007.2294](#), [doi:10.1016/j.physletb.2010.09.065](#).
- [20] H. Song, S. A. Bass, U. Heinz, T. Hirano, C. Shen, 200 A GeV Au+Au collisions serve a nearly perfect quark-gluon liquid, *Phys. Rev. Lett.* 106 (2011) 192301, [Erratum: *Phys. Rev. Lett.* 109,139904(2012)]. [arXiv:1011.2783](#), [doi:10.1103/PhysRevLett.106.192301](#), [doi:10.1103/PhysRevLett.109.139904](#).
- [21] H. Song, S. A. Bass, U. Heinz, Elliptic flow in 200 A GeV Au+Au collisions and 2.76 A TeV Pb+Pb collisions: insights from viscous hydrodynamics + hadron cascade hybrid model, *Phys. Rev. C* 83 (2011) 054912, [Erratum: *Phys. Rev. C* 87,no.1,019902(2013)]. [arXiv:1103.2380](#), [doi:10.1103/PhysRevC.83.054912](#), [doi:10.1103/PhysRevC.87.019902](#).
- [22] B. Schenke, S. Jeon, C. Gale, Anisotropic flow in $\sqrt{s} = 2.76\text{ TeV}$ Pb+Pb collisions at the LHC, *Phys. Lett. B* 702 (2011) 59–63. [arXiv:1102.0575](#), [doi:10.1016/j.physletb.2011.06.065](#).
- [23] C. Young, J. I. Kapusta, C. Gale, S. Jeon, B. Schenke, Thermally Fluctuating Second-Order Viscous Hydrodynamics and Heavy-Ion Collisions, *Phys. Rev. C* 91 (4) (2015) 044901. [arXiv:1407.1077](#), [doi:10.1103/PhysRevC.91.044901](#).

- [24] K. Murase, Causal hydrodynamic fluctuations and their effects on high-energy nuclear collisions, Ph.D. thesis, The University of Tokyo (2015). doi:10.15083/00072981.
URL https://repository.dl.itc.u-tokyo.ac.jp/?action=pages_view_main&active_action=repository_view_main_item_detail&item_id=47855&item_no=1&page_id=28&block_id=31
- [25] K. Murase, T. Hirano, Hydrodynamic fluctuations and dissipation in an integrated dynamical model, Nucl. Phys. A956 (2016) 276–279. arXiv:1601.02260, doi:10.1016/j.nuclphysa.2016.01.011.
- [26] M. Bluhm, M. Nahrgang, T. Schäfer, S. A. Bass, Fluctuating fluid dynamics for the QGP in the LHC and BES era, EPJ Web Conf. 171 (2018) 16004. arXiv:1804.03493, doi:10.1051/epjconf/201817116004.
- [27] M. Singh, C. Shen, S. McDonald, S. Jeon, C. Gale, Hydrodynamic Fluctuations in Relativistic Heavy-Ion Collisions, Nucl. Phys. A 982 (2019) 319–322. arXiv:1807.05451, doi:10.1016/j.nuclphysa.2018.10.061.
- [28] A. Sakai, K. Murase, T. Hirano, Rapidity decorrelation of anisotropic flow caused by hydrodynamic fluctuations, Phys. Rev. C 102 (6) (2020) 064903. arXiv:2003.13496, doi:10.1103/PhysRevC.102.064903.
- [29] K. Aamodt, et al., Elliptic flow of charged particles in Pb-Pb collisions at 2.76 TeV, Phys. Rev. Lett. 105 (2010) 252302. arXiv:1011.3914, doi:10.1103/PhysRevLett.105.252302.
- [30] K. Aamodt, et al., Higher harmonic anisotropic flow measurements of charged particles in Pb-Pb collisions at $\sqrt{s_{NN}}=2.76$ TeV, Phys. Rev. Lett. 107 (2011) 032301. arXiv:1105.3865, doi:10.1103/PhysRevLett.107.032301.
- [31] S. Chatrchyan, et al., Dependence on pseudorapidity and centrality of charged hadron production in PbPb collisions at a nucleon-nucleon centre-of-mass energy of 2.76 TeV, JHEP 08 (2011) 141. arXiv:1107.4800, doi:10.1007/JHEP08(2011)141.
- [32] G. Aad, et al., Measurement of the pseudorapidity and transverse momentum dependence of the elliptic flow of charged particles in lead-lead

- collisions at $\sqrt{s_{NN}} = 2.76$ TeV with the ATLAS detector, Phys. Lett. B707 (2012) 330–348. [arXiv:1108.6018](#), [doi:10.1016/j.physletb.2011.12.056](#).
- [33] A. Adare, et al., Measurements of Higher-Order Flow Harmonics in Au+Au Collisions at $\sqrt{s_{NN}} = 200$ GeV, Phys. Rev. Lett. 107 (2011) 252301. [arXiv:1105.3928](#), [doi:10.1103/PhysRevLett.107.252301](#).
- [34] J. Adam, et al., Azimuthal Harmonics in Small and Large Collision Systems at RHIC Top Energies, Phys. Rev. Lett. 122 (17) (2019) 172301. [arXiv:1901.08155](#), [doi:10.1103/PhysRevLett.122.172301](#).
- [35] G. Aad, et al., Measurement of the azimuthal anisotropy for charged particle production in $\sqrt{s_{NN}} = 2.76$ TeV lead-lead collisions with the ATLAS detector, Phys. Rev. C86 (2012) 014907. [arXiv:1203.3087](#), [doi:10.1103/PhysRevC.86.014907](#).
- [36] S. Chatrchyan, et al., Centrality dependence of dihadron correlations and azimuthal anisotropy harmonics in PbPb collisions at $\sqrt{s_{NN}} = 2.76$ TeV, Eur. Phys. J. C72 (2012) 2012. [arXiv:1201.3158](#), [doi:10.1140/epjc/s10052-012-2012-3](#).
- [37] F. G. Gardim, F. Grassi, M. Luzum, J.-Y. Ollitrault, Breaking of factorization of two-particle correlations in hydrodynamics, Phys. Rev. C87 (3) (2013) 031901. [arXiv:1211.0989](#), [doi:10.1103/PhysRevC.87.031901](#).
- [38] V. Khachatryan, et al., Evidence for transverse momentum and pseudorapidity dependent event plane fluctuations in PbPb and pPb collisions, Phys. Rev. C92 (3) (2015) 034911. [arXiv:1503.01692](#), [doi:10.1103/PhysRevC.92.034911](#).
- [39] M. Aaboud, et al., Measurement of longitudinal flow decorrelations in Pb+Pb collisions at $\sqrt{s_{NN}} = 2.76$ and 5.02 TeV with the ATLAS detector, Eur. Phys. J. C78 (2) (2018) 142. [arXiv:1709.02301](#), [doi:10.1140/epjc/s10052-018-5605-7](#).
- [40] P. Huo, Measurement of longitudinal flow correlations in Pb+Pb collisions at $\sqrt{s_{NN}} = 2.76$ and 5.02 TeV with the ATLAS detector, Nucl. Phys. A967 (2017) 908–911. [doi:10.1016/j.nuclphysa.2017.05.102](#).

- [41] M. Nie, Measurement of longitudinal decorrelation of anisotropic flow V_2 and V_3 in 200 GeV Au+Au collisions at STAR, Nucl. Phys. A982 (2019) 403–406. doi:10.1016/j.nuclphysa.2018.09.068.
- [42] G. Aad, et al., Longitudinal Flow Decorrelations in Xe+Xe Collisions at $\sqrt{s_{NN}} = 5.44$ TeV with the ATLAS Detector, Phys. Rev. Lett. 126 (12) (2021) 122301. arXiv:2001.04201, doi:10.1103/PhysRevLett.126.122301.
- [43] P. Bozek, W. Broniowski, J. Moreira, Torqued fireballs in relativistic heavy-ion collisions, Phys. Rev. C83 (2011) 034911. arXiv:1011.3354, doi:10.1103/PhysRevC.83.034911.
- [44] P. Bozek, W. Broniowski, Longitudinal decorrelation measures of flow magnitude and event-plane angles in ultrarelativistic nuclear collisions, Phys. Rev. C97 (3) (2018) 034913. arXiv:1711.03325, doi:10.1103/PhysRevC.97.034913.
- [45] B. Schenke, S. Schlichting, 3D glasma initial state for relativistic heavy ion collisions, Phys. Rev. C94 (4) (2016) 044907. arXiv:1605.07158, doi:10.1103/PhysRevC.94.044907.
- [46] Shen, Chun and Schenke, Björn, Dynamical initial state model for relativistic heavy-ion collisions, Phys. Rev. C97 (2) (2018) 024907. arXiv:1710.00881, doi:10.1103/PhysRevC.97.024907.
- [47] J. Jia, P. Huo, G. Ma, M. Nie, Observables for longitudinal flow correlations in heavy-ion collisions, J. Phys. G44 (7) (2017) 075106. arXiv:1701.02183, doi:10.1088/1361-6471/aa74c3.
- [48] A. Behera, M. Nie, J. Jia, Longitudinal eccentricity decorrelations in heavy ion collisions, Phys. Rev. Res. 2 (2) (2020) 023362. arXiv:2003.04340, doi:10.1103/PhysRevResearch.2.023362.
- [49] K. Xiao, F. Liu, F. Wang, Event-plane decorrelation over pseudorapidity and its effect on azimuthal anisotropy measurements in relativistic heavy-ion collisions, Phys. Rev. C 87 (1) (2013) 011901(R). arXiv:1208.1195, doi:10.1103/PhysRevC.87.011901.
- [50] L.-G. Pang, G.-Y. Qin, V. Roy, X.-N. Wang, G.-L. Ma, Longitudinal decorrelation of anisotropic flows in heavy-ion collisions at the CERN

- Large Hadron Collider, Phys. Rev. C91 (4) (2015) 044904. [arXiv:1410.8690](#), [doi:10.1103/PhysRevC.91.044904](#).
- [51] P. Bozek, W. Broniowski, The torque effect and fluctuations of entropy deposition in rapidity in ultra-relativistic nuclear collisions, Phys. Lett. B752 (2016) 206–211. [arXiv:1506.02817](#), [doi:10.1016/j.physletb.2015.11.054](#).
- [52] L.-G. Pang, H. Petersen, G.-Y. Qin, V. Roy, X.-N. Wang, Decorrelation of anisotropic flow along the longitudinal direction, Eur. Phys. J. A52 (4) (2016) 97. [arXiv:1511.04131](#), [doi:10.1140/epja/i2016-16097-x](#).
- [53] L.-G. Pang, H. Petersen, X.-N. Wang, Pseudorapidity distribution and decorrelation of anisotropic flow within the open-computing-language implementation CLVisc hydrodynamics, Phys. Rev. C97 (6) (2018) 064918. [arXiv:1802.04449](#), [doi:10.1103/PhysRevC.97.064918](#).
- [54] X.-Y. Wu, L.-G. Pang, G.-Y. Qin, X.-N. Wang, Longitudinal fluctuations and decorrelations of anisotropic flows at energies available at the CERN Large Hadron Collider and at the BNL Relativistic Heavy Ion Collider, Phys. Rev. C98 (2) (2018) 024913. [arXiv:1805.03762](#), [doi:10.1103/PhysRevC.98.024913](#).
- [55] L. D. Landau, E. M. Lifshitz, Fluid Mechanics, Pergamon Press, New York, 1959, sections 133–136.
- [56] E. M. Lifshitz, L. P. Pitaevskii, Statistical Physics Part 2, Butterworth-Heinemann, Oxford, 1980, sections 86–91.
- [57] E. Calzetta, Relativistic fluctuating hydrodynamics, Class. Quant. Grav. 15 (1998) 653–667. [arXiv:gr-qc/9708048](#), [doi:10.1088/0264-9381/15/3/015](#).
- [58] J. I. Kapusta, B. Muller, M. Stephanov, Relativistic Theory of Hydrodynamic Fluctuations with Applications to Heavy Ion Collisions, Phys. Rev. C85 (2012) 054906. [arXiv:1112.6405](#), [doi:10.1103/PhysRevC.85.054906](#).
- [59] K. Murase, T. Hirano, Relativistic fluctuating hydrodynamics with memory functions and colored noises (2013). [arXiv:1304.3243](#).

- [60] X. An, G. Basar, M. Stephanov, H.-U. Yee, Relativistic Hydrodynamic Fluctuations, *Phys. Rev. C* 100 (2) (2019) 024910. [arXiv:1902.09517](#), [doi:10.1103/PhysRevC.100.024910](#).
- [61] K. Murase, Causal hydrodynamic fluctuations in non-static and inhomogeneous backgrounds, *Annals Phys.* 411 (2019) 167969. [arXiv:1904.11217](#), [doi:10.1016/j.aop.2019.167969](#).
- [62] K. Murase, T. Hirano, Hydrodynamic fluctuations and dissipation in an integrated dynamical model, *Nucl. Phys. A* 956 (2016) 276–279. [arXiv:1601.02260](#), [doi:10.1016/j.nuclphysa.2016.01.011](#).
- [63] Y. Nara, N. Otuka, A. Ohnishi, K. Niita, S. Chiba, Study of relativistic nuclear collisions at AGS energies from p + Be to Au + Au with hadronic cascade model, *Phys. Rev. C* 61 (2000) 024901. [arXiv:nucl-th/9904059](#), [doi:10.1103/PhysRevC.61.024901](#).
- [64] T. Hirano, P. Huovinen, K. Murase, Y. Nara, Integrated dynamical approach to relativistic heavy ion collisions, *Progress in Particle and Nuclear Physics* 70 (2013) 108 – 158. [doi:https://doi.org/10.1016/j.ppnp.2013.02.002](#).
URL <http://www.sciencedirect.com/science/article/pii/S0146641013000045>
- [65] R. Baier, P. Romatschke, D. T. Son, A. O. Starinets, M. A. Stephanov, Relativistic viscous hydrodynamics, conformal invariance, and holography, *JHEP* 04 (2008) 100. [arXiv:0712.2451](#), [doi:10.1088/1126-6708/2008/04/100](#).
- [66] R. J. Glauber, Quantum optics and heavy ion physics, *Nuclear Physics A* 774 (2006) 3 – 13. [doi:https://doi.org/10.1016/j.nuclphysa.2006.06.009](#).
URL <http://www.sciencedirect.com/science/article/pii/S0375947406002399>
- [67] T. Sjostrand, S. Ask, J. R. Christiansen, R. Corke, N. Desai, P. Ilten, S. Mrenna, S. Prestel, C. O. Rasmussen, P. Z. Skands, An introduction to PYTHIA 8.2, *Comput. Phys. Commun.* 191 (2015) 159–177. [arXiv:1410.3012](#), [doi:10.1016/j.cpc.2015.01.024](#).

- [68] M. Okai, K. Kawaguchi, Y. Tachibana, T. Hirano, New approach to initializing hydrodynamic fields and mini-jet propagation in quark-gluon fluids, *Phys. Rev. C* 95 (5) (2017) 054914. [arXiv:1702.07541](#), [doi:10.1103/PhysRevC.95.054914](#).
- [69] K. Kawaguchi, K. Murase, T. Hirano, Multiplicity fluctuations and collective flow in small colliding systems, *Nucl. Phys. A* 967 (2017) 357–360. [doi:10.1016/j.nuclphysa.2017.07.010](#).
- [70] S. J. Brodsky, J. F. Gunion, J. H. Kuhn, Hadron Production in Nuclear Collisions: A New Parton Model Approach, *Phys. Rev. Lett.* 39 (1977) 1120. [doi:10.1103/PhysRevLett.39.1120](#).
- [71] A. Adil, M. Gyulassy, 3D jet tomography of twisted strongly coupled quark gluon plasmas, *Phys. Rev. C* 72 (2005) 034907. [arXiv:nucl-th/0505004](#), [doi:10.1103/PhysRevC.72.034907](#).
- [72] T. Hirano, U. W. Heinz, D. Kharzeev, R. Lacey, Y. Nara, Hadronic dissipative effects on elliptic flow in ultrarelativistic heavy-ion collisions, *Phys. Lett. B* 636 (2006) 299–304. [arXiv:nucl-th/0511046](#), [doi:10.1016/j.physletb.2006.03.060](#).
- [73] A. Bialas, M. Bleszynski, W. Czyz, Multiplicity Distributions in Nucleus-Nucleus Collisions at High-Energies, *Nucl. Phys. B* 111 (1976) 461–476. [doi:10.1016/0550-3213\(76\)90329-1](#).
- [74] J. D. Bjorken, Highly Relativistic Nucleus-Nucleus Collisions: The Central Rapidity Region, *Phys. Rev. D* 27 (1983) 140–151. [doi:10.1103/PhysRevD.27.140](#).
- [75] P. Huovinen, P. Petreczky, QCD Equation of State and Hadron Resonance Gas, *Nucl. Phys. A* 837 (2010) 26–53. [arXiv:0912.2541](#), [doi:10.1016/j.nuclphysa.2010.02.015](#).
- [76] F. Cooper, G. Frye, Comment on the Single Particle Distribution in the Hydrodynamic and Statistical Thermodynamic Models of Multiparticle Production, *Phys. Rev. D* 10 (1974) 186. [doi:10.1103/PhysRevD.10.186](#).
- [77] P. Kovtun, D. T. Son, A. O. Starinets, Viscosity in strongly interacting quantum field theories from black hole physics, *Phys. Rev. Lett.* 94

- (2005) 111601. [arXiv:hep-th/0405231](#), [doi:10.1103/PhysRevLett.94.111601](#).
- [78] H. Song, Causal Viscous Hydrodynamics for Relativistic Heavy Ion Collisions, Ph.D. thesis, Ohio State U. (2009). [arXiv:0908.3656](#).
- [79] K. Aamodt, et al., Centrality dependence of the charged-particle multiplicity density at mid-rapidity in Pb-Pb collisions at $\sqrt{s_{NN}} = 2.76$ TeV, *Phys. Rev. Lett.* 106 (2011) 032301. [arXiv:1012.1657](#), [doi:10.1103/PhysRevLett.106.032301](#).